

# COMPRESSIVE CONFOCAL MICROSCOPY

*P. Ye, J. L. Paredes, G. R. Arce, Y. Wu, C. Chen, D. W. Prather*

Department of Electrical and Computer Engineering  
University of Delaware, Newark, 19716, DE

## ABSTRACT

In this paper, a new framework for confocal microscopy based on the novel theory of compressive sensing is proposed. Unlike wide field microscopy or conventional parallel beam confocal imaging systems that use charge-coupled devices (CCD) as acquisition devices in addition to complex mechanical scanning system, the proposed compressive confocal microscopy is a kind of parallel beam confocal imaging system which exploits the rich theory of compressive sensing by using a single pixel detector and a digital micromirror device (DMD) to capture linear projections of the in-focus image. With the proposed system, confocal imaging of high optical sectioning ability can be achieved at sub-Nyquist sampling rates. Theoretical analysis, simulations and experimental results are shown to demonstrate the characteristics and potential of the proposed approach.

*Index Terms* — confocal imaging, compressive sensing, programmable array microscopy, SBHE, DMD

## 1. INTRODUCTION

Recently, the new field of compressive sensing (CS) has emerged with the promise to revolutionize digital signal/image processing broadly [1, 2]. The key idea is the use of non-adaptive linear projections to acquire an efficient, dimensionally reduced representation of a signal or image directly using just a few measurements. The recovered signals can be obtained from the compressed measurements using nonlinear reconstruction algorithms [3]. Such results can lead to the use of reduced resources at the acquisition stage of an imaging system, as that shown in [4] where random projections of an image are obtained using a single pixel detector. In essence, CS combines sampling and compression into a single non-adaptive linear measurement process, allowing sub-Nyquist sampling rate with no signal degradation.

This paper is motivated by the important realization that the fundamental principles governing confocal microscopy can be exploited almost effortlessly to attain the linear projections used in CS. Confocal microscopy is an imaging technique of increasing importance used in cell biology, genetics and microbiology [5]. Unlike conventional microscopy which images the whole field with one shot, confocal microscopy produces in-focus images through a process called

optical sectioning. Thus, images are captured in a point-by-point fashion and reconstructed by a software-driver. The key feature of confocal microscopy is the conjugate positioning of the source pinhole scanning point in the specimen and a second pinhole in front of a detector. It greatly reduces the out-of-focus light so that the axial resolution is significantly enhanced. Conventional confocal imaging, however, requires time-consuming scanning over 2D or 3D raster patterns. Several approaches to raster scanning have been introduced in order to speed-up the image acquisition time in confocal microscopy. In particular, architectures based on Programmable array microscopes (PAM) [6] are of great interest as these are based on coded illumination patterns readily attained by DMD. However, it is still limited by the Nyquist sampling rates.

In this paper, we exploit the rich theory of CS to reduce significantly the sampling rate and achieve, at the same time, perfect signal reconstruction. Compressive sensing fundamentally relies on the sampling of random projections. Thus, rather than measuring the contribution of a single pinhole as it is sequentially scanned, the proposed compressive confocal microscopy measures the superposed contributions of a random set of pinholes, using only a single detector. Given a small set of measurements, each with a different arrangement of pinholes, the theory of compressed sensing then allows for the perfect image reconstruction from a dimensionally reduced representation. Compressive confocal microscopy (CM) emerges as a new CM framework offering the potential advantage to lowering costs by simplifying the hardware and optical complexity. This is attained by off-loading the processing from the data acquisition into the image reconstruction which is performed digitally in a standard computer.

## 2. COMPRESSIVE CONFOCAL MICROSCOPY

In the proposed compressive confocal CM, a DMD placed at the primary image plane is uniformly illuminated by coherent or incoherent light source. The modulation pattern of the DMD produces a structured illumination on the object as is shown in Fig. 1. The emission (or reflection) light from the object is then imaged back onto the DMD and from there, via a beam splitter and focusing lens, onto a single pixel detector. By adding up the contributions from all micromirrors at the 'on' position, we get the conjugate measurement, which

is formed by the ‘in-focus’ light[6] and is a linear projection of the in-focus plane. The system we are studying is an incoherent optical system, thus the objective could be modeled as a linear translation invariant (LTI) system of intensity. Three-dimensional (3D) imaging is realized by moving the object along the axial direction and obtaining CS measurements of the corresponding slice at the in-focus plane. As can be seen in Fig. 1 no mechanical scanning is needed in the imaging process since the single pixel detector is fixed in the lateral dimension. Furthermore, by changing the orientation of the micromirrors several projections of the in-focus plane can be obtained.

Next, we derive the expression for the compressive CM measurement in fluorescence mode. Following the definition in [6], the  $i$ -th modulation pattern of a DMD is given by

$$S_i(x_d, y_d) = \begin{cases} 1 & \text{if } (x_d, y_d) \text{ is on a mirror that is 'on'} \\ 0 & \text{if } (x_d, y_d) \text{ is on a mirror that is 'off'} \end{cases} \quad (1)$$

where  $(x_d, y_d)$  is the two-dimensional (2D) coordinate system on DMD plane, with  $(0, 0)$  as the center of DMD. It can be shown that the illumination pattern of a given object is given by

$$I_{ex}(x_o, y_o, z_o; i) = \iint_{-\infty}^{+\infty} S_i(Mu, Mv) \times H_{ex}(x_o - u, y_o - v, z_o) dudv, \quad (2)$$

where  $M$  and  $H_{ex}$  are, respectively, the magnification and the excitation point spread function (PSF) of the objective.  $(x_o, y_o, z_o)$  denotes a 3D coordinate system for the object  $O(x_o, y_o, z_o)$ , where  $x_o = \frac{x_d}{M}$ ,  $y_o = \frac{y_d}{M}$ .

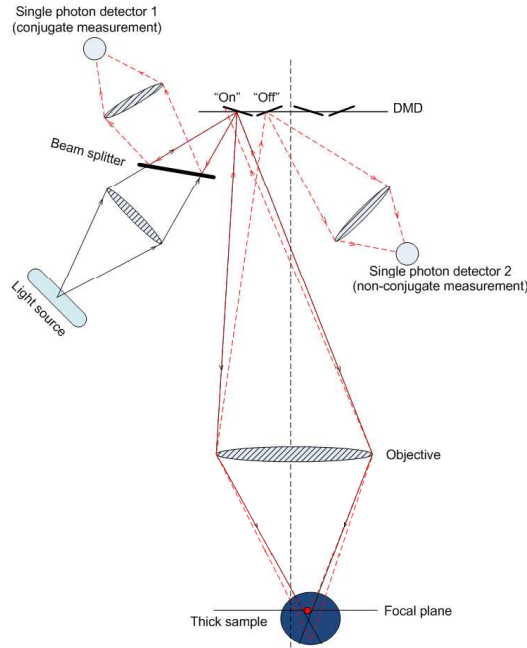


**Fig. 1.** Compressive confocal microscopy system.

The  $i$ -th conjugate measurement is given by adding up the contribution of reflected light off mirror elements at the ‘on’ position. This is,

$$I_c(i) = \int_{-\frac{L \times \rho}{2}}^{\frac{L \times \rho}{2}} \int_{-\frac{W \times \rho}{2}}^{\frac{W \times \rho}{2}} \iint_{-\infty}^{+\infty} H_{em}\left(\frac{x_d}{M} - u, \frac{y_d}{M} - v, w\right) \times I_{ex}(u, v, w; i) O(u, v, w - z_s) dudvdw \times S_i(x_d, y_d) dx_d dy_d, \quad (3)$$

where  $L$  and  $W$  mean that there are  $L \times W$  micromirrors on the DMD,  $\rho$  is the size of DMD mirror,  $H_{em}$  is the emission PSF of the objective. The non-conjugate measurement from the mirror elements at ‘off’ position, which is formed by ‘out-of-focus’ light, is given by

$$I_n(i) = \int_{-\frac{L \times \rho}{2}}^{\frac{L \times \rho}{2}} \int_{-\frac{W \times \rho}{2}}^{\frac{W \times \rho}{2}} \iint_{-\infty}^{+\infty} H_{em}\left(\frac{x_d}{M} - u, \frac{y_d}{M} - v, w\right) \times I_{ex}(u, v, w; i) O(u, v, w - z_s) dudvdw (1 - S_i(x_d, y_d)) dx_d dy_d, \quad (4)$$

For mathematical tractability, we assume a discrete model for the object of interest. More precisely, to reconstruct an  $N \times N$  object  $f(m, n)$ ,  $m = 1, 2, \dots, N$ ;  $n = 1, 2, \dots, N$ , the DMD is divided into  $N \times N$  cells, with  $\frac{W}{N} \times \frac{L}{N}$  mirrors in one cell. In the process of imaging, each mirrors within one cell are set at the same position, i.e. all ‘on’ or all ‘off’. Let  $S_i(m, n)$  represent the status of the  $(m, n)$ -th cell for the  $i$ -th measurement, then we have:

$$I_c(i) = \sum_{m=1}^N \sum_{n=1}^N S_i(m, n) C_i(m, n) f(m, n) + I_{c,blur}(i) + \mathbf{b}_c(i), \quad (5)$$

$$I_n(i) = \sum_{m=1}^N \sum_{n=1}^N S_i(m, n) (I_{ex,i}(m, n) - C_i(m, n)) f(m, n) + I_{n,blur}(i) + \mathbf{b}_n(i), \quad (6)$$

where  $C_i(m, n)$  represents the percentage of collected energy at the  $(m, n)$ -th point for the  $i$ -th modulation pattern,  $I_{ex,i}(m, n)$  represents the illumination on the  $(m, n)$ -th point ( $0 \leq I_{ex,i}(m, n) \leq 1$ ),  $I_{c,blur}(i)$  and  $I_{n,blur}(i)$  are contributions from points at focal plane conjugate to ‘off’ mirrors,  $\mathbf{b}_n(i)$  and  $\mathbf{b}_c(i)$  represent out-of-focus contributions (background). Ideally,  $C_i(m, n) = \delta(S_i(m, n) - 1)$ . However, due to the effect of PSF, light arising from conjugate point on object will leak some energy on its neighbor points. If the neighbor point is also ‘on’, then the leaked energy will still be collected by conjugate measurement detector. If the neighbor point is ‘off’, the energy will not be detected by conjugate measurement detector, which means  $C_i(m, n) < 1$  when  $S_i(m, n) = 1$ .  $C_i(m, n)$  can be thought of as impulse response of the system, it varies with position  $(m, n)$  and ‘acquisition time’  $i$ .

The modulation patterns given by Eq. (1) has to be defined in some optimal fashion, since it incorporates the randomness needed to project the image of interest into a random basis. To be more precise, consider a 2D image  $F$  of size

$N \times N$ ,  $F = \{f(m, n)\}$ ,  $n = 1, 2, \dots, N$ ;  $m = 1, 2, \dots, N$ . Furthermore, suppose  $F$  is sparse or compressible on some fixed basis. Let  $\Phi$  be a  $N \times N$  random binary sensing matrix. Projecting  $F$  onto  $\Phi$  yields:  $Y = \Phi F \Phi^H$ , where  $Y = \{y(m, n)\}$ ,  $m = 1, 2, \dots, N$ ;  $n = 1, 2, \dots, N$ . It can be shown that the projection operation reduces to:

$$y(m, n) = \langle B^{m,n}, F \rangle, \quad (7)$$

$\{B^{m,n}\}$  is referred to as measurement ensemble. Among the  $N^2$  projections, we randomly choose  $M$  ( $M < N^2$ ) possible modulation patterns that leads to  $M$   $\{B^{m,n}\}$  measurement matrices. Loading the  $M$  basis images  $B$  onto the DMD with mirror elements switched to 'on' ('off') position if the corresponding entry on the  $B$  matrix is a 1 (0). We obtain thus a collection of  $M$  measurements. Then, we proceed to reconstruct  $F$  via non-linear optimization from the  $M$  measurements [3]. Two different sensing systems that have been found to speed up the signal reconstruction process are used to define the modulation pattern  $\{B^{m,n}\}$ . They are Ordered Hadamard ensemble (ODHE) and Scrambled Block Hadamard ensemble (SBHE) [7].

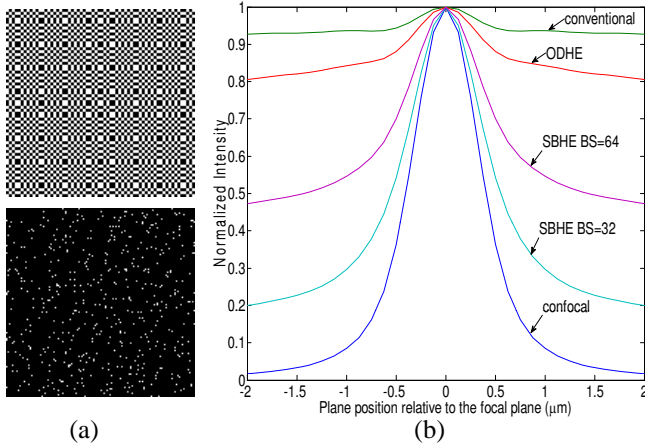


**Fig. 2.** (a) Example of modulation patterns, image size  $128 \times 128$ . Top: ODHE, percentage of openings 50%. Bottom: SBHE, BS=32, percentage of openings 3.125%. (b) The conjugate measurement of an infinitely thin plane as a function of its relative position to the in-focus plane obtained by compressive CM with several modulation patterns. The system parameters are set as follows: DMD micromirror size  $\rho = 13.68 \mu\text{m}$ , NA=1.4, M=100, excitation wavelength=633nm, emission wavelength=665nm, refractive index=1.515.

For ODHE pattern, the measurement matrix  $B^{m,n}$  is defined as  $B^{m,n} = H Z^{m,n} H^T$ , where  $H$  is the Hadamard transform matrix and  $Z^{m,n}$  is an  $N \times N$  matrix with just a non-zero entry at position  $(m, n)$ . Note that  $B^{m,n}$  contains a basis of the Hadamard transform. In turn, the 'on' mirrors are placed closely and not pure randomly on DMD,  $C_i(m, n)$  is thus spatial-variant, which may cause severe artifacts at the corner of the reconstructed image from conjugate measurement.

As can be seen in Eq. (6), non-conjugate measurements contains those 'leaked' energy from conjugate points. We could minimize those artifacts by adding up recovered images from non-conjugate measurement to it.

For SBHE patterns,  $B^{m,n} = P_N^{-1} W^{-1} Z^{m,n}$ , where  $Z^{m,n}$  is a matrix with just one non-zero entry at the  $(m, n)$  position,  $P_N$  represents  $N^2$  points scramble operator and  $W$  is a block Hadamard transform operator [7]. Since SBHE pattern is sparse, it is quite likely that neighbor mirrors of an 'on' mirror are all set to 'off' position. Under this assumption,  $C_i(m, n)$  in Eq. (5) could be considered as spatial-invariant. Furthermore, the distribution of 'on' mirror in SBHE pattern is pure random and the percentage of openings are the same for all the measurements (except for measurements corresponding to the lowest frequency components in the Hadamard domain),  $C_i(m, n)$  is also time-invariant.

Figure 2 (a) depicts illustrative examples of an ODHE and an SBHE measurement matrices. As can be seen, the SBHE pattern is much sparser than the ODHE pattern. In turn, the light efficiency becomes much lower. Figure 2(b) shows the normalized axial response of an infinitely thin plane with different modulation patterns. As can be seen from Figure 2(b), the SBHE pattern offers better optical sectioning ability than the ODHE pattern. The improvement in degree of confocality found arises from the sparsity of SBHE pattern. Thus there is a tradeoff between light efficiency and optical sectioning ability, thus by increasing the block size (BS) of the SBHE pattern, light efficiency increases whereas the degree of confocality decreases.

### 3. SIMULATIONS

In Fig. 3, we evaluate the performance of the compressive CM as the object thickness changes. The performance of the proposed approach is compared to that yielded by conventional microscopy. Equations (3) and (4) are used to model the imaging system numerically. PSF for the simulation is generated by ImageJ Plug-in Diffraction PSF 3D [8]. Figure 3(b) shows images from compressive CM with ODHE patterns obtained by subtracting recovered nonconjugate image from the recovered conjugate image. Figure 3(b) shows images from compressive CM with SBHE patterns reconstructed using conjugate measurement only. These results show that as the object thickness increases, due to poor optical sectioning ability, the quality of the reconstructed images obtained with conventional microscopy and compressive CM with ODHE starts to degrade, whereas, as shown in Figure 2(b), compressive CM with SBHE yields much better sectioning capability offering thus higher quality image for thick object compared to that of conventional microscopy. Note that the performance of compressive CM with ODHE is competitive compared to that yielded by conventional microscopy. For CS image reconstruction, we use total variation minimization algorithm.

### 4. EXPERIMENTAL RESULTS

To evaluate the performance of the proposed compressive CM in a practical scenario, we design a hardware prototype

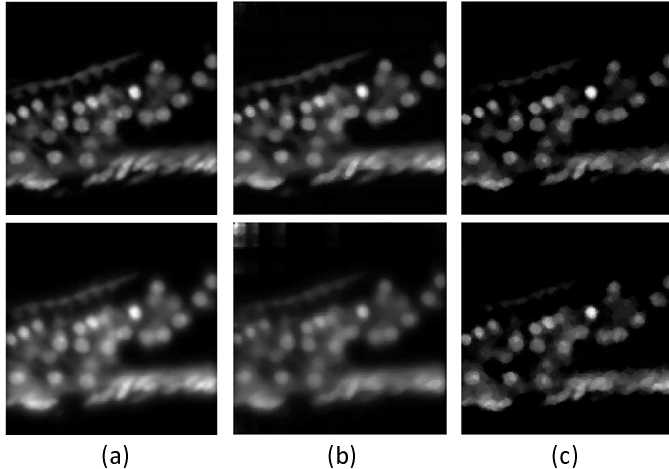


**Fig. 3.** (a) Conventional wide-field imaging. (b) Compressive CM with ODHE pattern. (c) Compressive CM with SBHE pattern, BS=32. Simulation parameters: micromirror size  $\rho = 13.68\mu\text{m}$ , NA=1.4, refractive index=1.515, excitation wavelength=633nm, emission wavelength=665nm, DMD size  $1024 \times 768$ , sampling rate=25%, image size= $128 \times 128$ . Top: thickness= $0.14\mu\text{m}$ . Bottom: thickness  $7\mu\text{m}$ .

(testbed) that uses low cost and widely available components. In the experimental setup, shown in Fig. 4(b), the objective used has a magnification of 40 and 0.63 NA. A DC regulated quartz halogen lamp is used as illumination source. The source is collimated and projected to a Texas Instruments DMD of up to  $1024 \times 768$   $13.68 \times 13.68 \mu\text{m}^2$  mirrors optimized at the visible spectrum. Figure 4(a) depicts the reconstructed images yielded by the  $l_1$  regularized least square algorithm [3] with real data captured using the experimental setup for two different modulation patterns with a compression rate of 45%. Note that, the imaging target here is infinitely thin and compressive CM works in reflection mode. In this case, compressive CM with ODHE and SBHE pattern yield comparative performance in agreement with the simulation results of an thin object with thickness  $0.14\mu\text{m}$ .

## 5. CONCLUSIONS

In this paper, we have developed a new confocal microscopy system based on compressive sensing. The proposed compressive CM has the potential advantage of simplifying the hardware and optical complexity of confocal imaging systems by off-loading the processing from the data acquisition stage into that of image reconstruction which is software driven leading thus to a lower-cost imaging system. Furthermore, it offers the unique optical sectioning property of confocal imaging. Depending on the design of compressive sampling measurement patterns (illumination patterns), in some cases up to 90% reduction of scan effort and 50% light efficiency are feasible. To fully explore this design concept, our future work will be focused on: develop system noise cancelations, test compressive CM with biological specimens, design optimal projection matrices and explore 3D reconstruction.

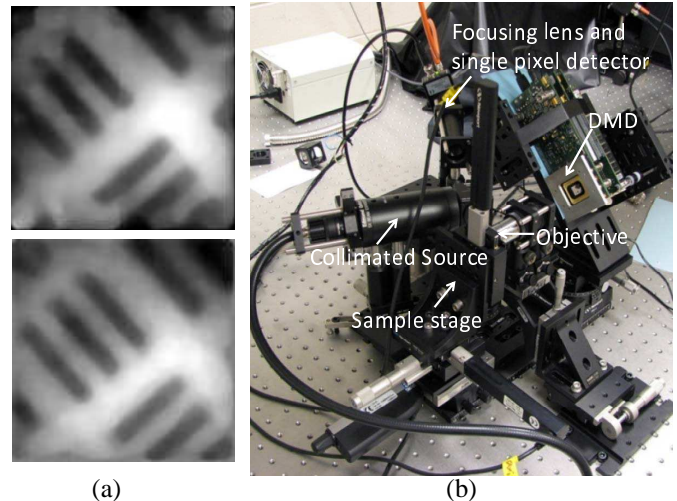


**Fig. 4.** Confocal images reconstructed using projections obtained from the experimental testbed. Image reconstruction obtained from (a) Top: ODHE projection patterns and (a) Bottom: SBHE projection patterns, BS=64. For both the sampling rate=45%, image size= $128 \times 128$ . Imaging target: USAF-1951, group 5, element 4,  $45.25 \text{ lp/mm}$ , feature size  $11\mu\text{m}$  (b) Experimental setup.

## 6. REFERENCES

- [1] E. Candés, J. Romberg, and T. Tao, “Robust uncertainty principles: Exact signal reconstruction from highly incomplete frequency information,” *IEEE Trans. Information Theory*, vol. 52, pp. 489–509, 2006.
- [2] E. Candés and T. Tao, “Near-optimal signal recovery from random projections and universal encoding strategies?,” *IEEE Trans. Information Theory*, vol. 52, pp. 5406–5245, 2006.
- [3] K. Koh, S. Kim, and S. Boyd, “l1\_ls : A matlab solver for large-scale l1-regularized least squares problems,” Stanford University, Mar. 2007.
- [4] M.F. Duarte, M.A. Davenport, D. Takhar, J.N. Laska, T. Sun, K.F. Kelly, and R.G. Baraniuk, “Single-pixel imaging via compressive sampling,” *IEEE Signal Processing Magazine*, March 2008.
- [5] T. Wilson, *Confocal Microscopy*, Academic Press, 1990.
- [6] P. J. Verveer, Q. S. Hanley, P. W. Verbeek, L. J. van Vliet, and T. M. Jovin, “Theory of confocal fluorescence imaging in the programmable array microscope (pam),” *J. Opt. Soc. Am.*, vol. 3, pp. 192–198, 1998.
- [7] L. Gan, T. T. Do, and T. D. Tran, “Fast compressive imaging using scrambled block hadamard ensemble,” 2008, Preprint.
- [8] Bob Dougherty, “Diffraction psf 3d,” 2005, Online, <http://www.optinav.com/Diffraction-PSF-3D.htm>.